Published in final edited form as:
Brain Res. 2011 September 30; 1415: 34–46. doi:10.1016/j.brainres.2011.07.024.

Comparison of CRF-immunoreactive neurons distribution in mouse and rat brains and selective induction of Fos in rat hypothalamic CRF neurons by abdominal surgery

Lixin Wang[*], **Miriam Goebel-Stengel**[*], **Andreas Stengel**, **S. Vincent Wu**, **Gordon Ohning**, and **Yvette Taché**
CURE:Digestive Diseases Research Center and Center for Neurobiology of Stress, Department of Medicine, Division of Digestive Diseases, University of California Los Angeles, VAGLAHS, Los Angeles, California 90073, USA.

Abstract

Mice and rats are widely used in stress-related behavioral studies while little is known about the distribution of the stress hormone, corticotropin-releasing factor (CRF) in the mouse brain. We developed and characterized a novel rat/mouse CRF polyclonal antibody (CURE ab 200101) that was used to detect and compare the brain distributions of CRF immunoreactivity in naïve and colchicine-treated rats and mice. We also assessed whether the visceral stressor of abdominal surgery activated brain CRF neurons using double labeling of Fos/CRF in naïve rats. CRF-ir neurons were visualized in the cortex, bed nucleus of the stria terminalis, central amygdala, hypothalamic paraventricular nucleus (PVN), Barrington's nucleus and dorsolateral tegmental area in naïve rats. CRF-immunoreactive (ir) neurons in the mouse brain were detected only after colchicine. The pattern shows fundamental similarity compared to the colchicine-treated rat brain, however, there were differences with a lesser distribution in both areas and density except in the lateral septum and external subnucleus of the lateral parabrachial nucleus which contained more CRF-ir neurons in mice, and CRF-ir neurons in the dorsal motor nucleus of the vagus were found only in mice. Abdominal surgery in naïve rats induced Fos-ir in 30% of total CRF-ir neurons in the PVN compared with control (anesthesia alone) while Fos was not co-localized with CRF in other brain nuclei. These data indicate that CRF-ir distribution in the brain displays similarity as well as distinct features in mice compared to rats that may underlie some differential stress responses. Abdominal surgery activates CRF-ir neurons selectively in the PVN of rats without colchicine treatment.

Keywords

Corticotropin-releasing factor; CRF antibody; Fos; paraventricular nucleus of the hypothalamus; dorsal motor nucleus of the vagus; abdominal surgery; rat; mouse

Address for correspondence: Lixin Wang, MD, PhD, Bldg. 115, Rm. 117B, 11301 Wilshire Blvd, Los Angeles, CA 90073, USA, Tel.: 310 478 3711 ex 41831, Fax: 310 268 4963, lixinw@ucla.edu.
[*]Equal contribution

1. Introduction

The corticotropin-releasing factor (CRF) family of peptides includes fish urotensin-I, amphibian sauvagine, and mammalian peptides, CRF and urocortin (Ucn) 1, Ucn 2 and Ucn 3 (Hauger et al., 2003; Lovejoy et al., 2009; Lovejoy and Balment, 1999). The primary structure of CRF, a 41 amino acid peptide, is highly conserved across mammalian species with 100% sequence homology among rat, mouse and human (r/m/hCRF; accession numbers: rat: AAA40965.1; mouse: AAI19037.1; human: AAH02599.1 – aa 145–185). Likewise, the 40 amino acids peptide, Ucn 1 is identical between rats and mice, and rodent Ucn 1 and CRF share 18 out of 40 residues in their C-terminal biologically active forms (Lovejoy and Balment, 1999; Seasholtz et al., 1991; Vaughan et al., 1995). Convergent reports have established that the brain CRF system plays a pivotal role in orchestrating the stress response (Bale and Vale, 2004; Stengel and Taché, 2010). In particular, brain CRF is involved in acute stress-related alterations in behavior, energy balance, endocrine, cardiovascular, immune and gastrointestinal functions (Bale and Vale, 2004; Fekete and Zorrilla, 2007; Owens and Nemeroff, 1991; Taché and Bonaz, 2007).

CRF pleiotropic central actions are associated with its wide brain distribution not only in the hypothalamo-hypophyseal axis (paraventricular nucleus, PVN-median eminence) but also in extrahypothalamic circuits, namely the cerebral cortex, limbic system [hippocampus, central nucleus of the amygdala (CeA) and bed nucleus of the stria terminalis (BST)], and specific nuclei in hindbrain (Cummings et al., 1983; Merchenthaler et al., 1982; Morin et al., 1999; Olschowka et al., 1982; Petrusz et al., 1985; Sawchenko and Swanson, 1990; Sawchenko et al., 1993; Skofitsch and Jacobowitz, 1985; Swanson et al., 1983) as amply documented in rats treated with colchicine. By contrast, detailed mapping of brain CRF immunoreactivity in mice compared to Ucn 1 (Weitemier et al, 2005) is not available besides the distribution of CRF mRNA expression in wild type mouse brain for comparison with that of green fluorescent protein under the control of CRF gene promoter (Alon et al., 2009). The paucity of information on distribution of CRF immunoreactivity in murine brain is at variance with numerous mouse models genetically modified, including components of CRF signaling system (Coste et al., 2001; Elliott et al., 2010) used to perform behavioral or functional stress-related studies (Delic et al., 2008; Pollak et al., 2010). Physiological investigations in mice on the role of brain CRF signaling circuitries are usually largely interpreted based on the knowledge of CRF immunoreactivity distribution in rat brain. However, while similarly to rats, CRF-immunoreactive (ir) cell bodies are detected in mouse PVN (Westberg et al., 2009; Workman et al., 2008), one detailed comparative analysis of the CRF-ir system focused on the CeA points to some drastic differences in the labeling fiber density in CeA subnuclei between rats and mice (Asan et al., 2005). Therefore, the present study was designed to map the localization of CRF-containing neurons throughout the mouse brain compared to that in the rat with or without treatment with the axonal transport blocker, colchicine known to induce accumulation of neuropeptides in the somata of projecting neurons and thus improving their visualization. CRF immunostaining was performed using a newly developed polyclonal r/m/hCRF antibody (CURE ab 200101) that was characterized by binding test, immunodot blot, immunohistochemistry with pre-absorptions of the antibody by CRF family peptides in established rat brain nuclei, and comparison with another commonly used rabbit anti-r/hCRF serum (#PBL rC70, Salk Institute) (Sawchenko et al., 1984) and the r/mUcn 1 antibody (CURE ab 2023).

Of relevance to define stress-related brain circuitries is the ability to use Fos as a marker of neuronal activation (Morgan and Curran, 1991) with double immunolabeling with CRF. Under stress-related conditions, colchicine cannot be used to enhance the detection of CRF immunolabeling as it constitutes in itself a strong stressful stimulus resulting in Fos induction in the brain (Berkenbosch and Tilders, 1988; Bittencourt et al., 1999; Ceccatelli et

al., 1989; Kainu et al., 1993; Mundy and Tilson, 1990). In addition, we found that in mouse brain very few CRF-ir neurons can be detected without colchicine treatment, and double immunostaining of Fos and CRF has been almost exclusively performed in rats. In particular, activation of CRF neurons was demonstrated in response to novel environment, immobilization, immune challenge and sodium nitroprusside-induced hypotension mainly in the PVN, and in limited studies, in the CeA, Barrington's nucleus and dorsal lateral BST of rats (Crane et al., 2005; Curtis et al., 2002; Rivest and Rivier, 1994; Rotllant et al., 2007). We previously reported that abdominal surgery induces prominent Fos expression in the PVN and hindbrain nuclei as monitored 1 to 3 h after abdominal surgery (Barquist et al., 1996; Bonaz et al., 1994; Stengel et al., 2010). Functional studies also indicate that activation of brain CRF receptors is involved in the delayed gastric emptying occurring in the immediate phase post abdominal surgery in rats and mice (Barquist et al., 1996; Bonaz et al., 1994; Luckey et al., 2003; Taché et al., 1991). In this study, we further assessed whether brain nuclei expressing CRF immunoreactivity in non colchicine treated rats were activated by abdominal surgery to identify CRF brain circuitries recruited by such a visceral stressor.

2. Results

2.1. Specificity of rabbit anti-r/m/h CRF polyclonal antibody, CURE 200101

In radioimmunoassay studies, the CRF polyclonal antibody CURE 200101 showed specific linear binding to r/m/hCRF (ID_{50}: 4.7 ng/ml) and cross reaction with fish urotensin-I (ID_{50}: 30 ng/ml) but not with r/mUcn 1, mUcn 2, mUcn 3 or frog sauvagine (ID_{50}: >100 ng/ml, Fig. 1A). By immunodot blot, the CRF antibody (1:10,000) showed immunoreactivity only to r/m/hCRF, but not to urotensin-I, sauvagine, r/mUcn 1, mUcn 2 and mUcn 3 or bovine serum albumin (BSA) using 500 ng/blot of each peptide (Fig. 1B).

Immunohistochemistry studies in mouse and rat brains treated with colchicine using the CRF antibody CURE 200101 showed that the visualized CRF immunoreactivity was completely abolished by pre-absorption of the antibody with CRF in both mouse and rat brains as illustrated in the rat PVN, CeA and Edinger-Westphal (EW) nuclei (Fig. 2) and in the mouse PVN (Supplemental Fig. S1) except some fibers in the median eminence (not shown). Pre-absorption with other CRF family peptides revealed cross-reactivity of the antibody with fish urotensin-I > r/mUcn 1 > mUcn 2 and no cross-reactivity with mUcn 3 and sauvagine in rat brain sections (Fig. 2 and Fig. S1).

We also validated the CRF antibody CURE 200101 in colchicine-treated rats and mice by comparing the distribution of CRF staining to that obtained with another commonly used rabbit anti-r/hCRF serum, PBL rC70 (Sawchenko et al., 1984) simultaneously processed as CURE ab 200101. The two antibodies showed by in large similar CRF-ir distribution in the mouse and rat brains. Few differences were found related to rC70 labeling of CRF-ir neurons in the rat hypoglossal nucleus and nucleus ambiguous, and displaying higher background in some nuclei, such as the suprachiasmatic and arcuate nucleus of the hypothalamus (data not shown).

Since CRF ab 200101 partially cross-reacted with Ucn 1 as shown in the rat PVN and CeA, and there was a total absence of CRF immunoreactivity in the EW after pre-absorption with Ucn 1 (Fig. 2), we also performed immunohistochemistry for Ucn 1-ir neurons in the rat brain sections using the r/mUcn 1 antibody (CURE ab 2023) generated under the same conditions as the CRF antibody. The antibody did not show cross reaction by immunohistochemistry with r/m/hCRF, mUcn 2, mUcn 3, frog sauvagine and fish urotensin-I (Supplementary Fig. S2), and displayed the same selective distribution in rat brain including high immunoreactivity especially in the EW (Supplementary Fig. S2) as previously reported (Bittencourt et al., 1999; Kozicz et al., 1998; Morin et al., 1999).

2.2. Distribution of CRF-ir neurons in the brain of naïve and colchicine-treated rats

In naïve rats without colchicine treatment, the distribution of neuronal cytoplasm labeled with CRF immunoreactivity was found in selective brain areas. Namely, the PVN displayed the most abundant CRF-labeled neurons. Other areas included the cortex, namely the prefrontal, cingulate and sensorimotor cortex, BST (lateral division, dorsal part), CeA (lateral division), Barrington's nucleus and dorsolateral tegmental area (DLTg) (Fig. 3A–D). The intracerebroventricular (icv) colchicine injection at a low dose (20 μg/rat) enhanced CRF-labeled neurons in rat brain nuclei as summarized in Table 1. Besides the intensively labeled neurons in the PVN (Fig. 2), the medial preoptic area (Fig. 4A), BST, CeA (Fig. 2), lateral mammillary nucleus (Fig. 3F), Barrington's nucleus and DLTg (Fig. 3H) contained moderate numbers of CRF-ir neurons. Other areas bearing significant CRF-ir neurons included the cortex (same distribution as without colchicine treatment), perifornical and lateral hypothalamic areas (Fig. 3E), EW (Fig. 2), lateral periaqueductal gray (PAG), ventral-median PAG (Fig. 3G), lateral parabrachial nucleus (LPB; Fig. 4E), subcoeruleus (Fig. 3H), external cuneate nucleus and superior paraolivary nucleus (not shown). The CRF-ir neurons in the ventral-median PAG (Fig. 3G) consisted of a small but compact group of CRF-ir neurons ventral to the cerebral aqueduct in the midline of PAG at the rostral level of the dorsal raphe.

2.3 Distributions of CRF-ir nerve fibers in the brain of naïve rats

In naïve rats, CRF-ir fibers were observed in selective brain areas (Table 1). The highest density was found in the external lamina of the median eminence, high density in the piriform cortex, BST, CeA, dorsal raphe, midbrain reticular formation, area postrema and nucleus of the solitary tract, and moderate density in the lateral and dorsomedial hypothalamic areas, PAG, medial parabrachial nucleus and LPB, external cuneate nucleus and inferior olivary nuclei. The hypophysiotropic projecting fibers from the PVN to the median eminence were well traced with CRF-ir around the fornix and in the retrochiasmatic area where they gathered in a bundle. Another characteristic feature was found in the cerebellar cortex with abundant CRF immunoreactivity in the climbing and mossy fibers.

2.4. Brain distribution of CRF-ir neurons and fibers in naïve and colchicine treated mice and differences between mice and rats

Mouse brains without colchicine treatment showed only scattered CRF-ir neurons in the cortex. The comprehensive listing of CRF-ir neurons in specific nuclei throughout the brain of mice injected icv with colchicine at a similar dose as in rats and that of CRF-ir fibers in naïve mice is detailed in Table 1. CRF immunoreactivity distribution analysis in the mouse brain compared to the rat shows fundamental similarity, however, there were differences related to the lesser distribution in both, areas and density. The most numerous CRF-ir neurons in the mouse brains treated with colchicine were observed in the PVN, and moderate expression was found in the lateral septum, BST, CeA, EW, external subnucleus of the LPB (Fig. 4F), Barrington's nucleus and the dorsal motor nucleus (DMN) of the vagus (Fig. 4H). The major differences between rats and mice were the numerous CRF-ir neurons in the medial preoptic area of rats that were barely observed in mice (Fig. 4A, B). By contrast, CRF-ir neurons in the lateral septum and the external subnucleus of the LPB were more densely expressed in mice than rats (Fig. 4 E, F). In addition, mice displayed CRF-ir neurons in the DMN which were not found in rats (Fig. 4G, H).

CRF-ir fibers in naïve mice were prominent in the median eminence, BST and CeA and moderately in the medial preoptic area, several midbrain nuclei (PAG, lateral part of substantia nigra, dorsal raphe, ventral tegmental area) and a few in pontine and medullary nuclei (the medial parabrachial nucleus, ventrolateral medulla and inferior olivary nuclei) (Table 1).

2.5. Activation of CRF-ir neurons by abdominal surgery in rats

After abdominal surgery consisting of laparotomy and 1 min cecal manipulation or sham operation (anesthesia alone for 8 min), CRF-ir neurons were displayed in the PVN in rats without colchicine treatment. The number of single labeled CRF-ir neurons in the PVN 2-h after abdominal surgery was significantly decreased by 25% compared to sham (cells/section: 66.9 ± 2.6 *vs.* 89.0 ± 6.6; $p < 0.05$; Fig. 5D). Abdominal surgery induces an increase in Fos expression at 2 h post-surgery in the PVN as shown by the increase in the number of Fos-ir neurons/section compared to the sham group (cells/section: 205.4 ± 18.5 *vs.* 23.5 ± 6.2; $p < 0.001$, Fig. 5A). Fos-ir cells were mainly located in the parvicellular division of the PVN where the majority of CRF-ir neurons were detected (Fig. 5B, C). Other brain nuclei containing CRF-ir neurons in non-colchicine-treated rats, such as the BST, CeA and Barrington's nucleus had a few Fos-ir cells 2-h after surgery or sham procedure, and did not show co-localization with CRF as illustrated in the BST (Fig. 5E, F, and data not shown). Abdominal surgery significantly increased the number of double labeled cells in the PVN compared to sham treatment (48.6 ± 5.5 *vs.* 14.8 ± 5.6, $p < 0.01$, Fig. 5B and D). Of the Fos-ir neurons induced by abdominal surgery, 23.7% were also CRF-ir and of the total CRF-ir neurons, 30% were activated as shown by double immunolabeling of Fos and CRF (Fig. 5D).

3. Discussion

The current immunohistochemical study documents the first mapping of CRF-ir neurons and fibers in the brain of C57BL/6 mice in comparison with Sprague Dawley rats in naïve and colchicine-treated animals. This was achieved by using the novel r/m/hCRF antiserum CURE 200101 generated by stabilized CRF ($DTyr^{0}CRF$) peptide that yields good quality of immunostaining and a similar pattern of CRF-ir neuronal distribution in the rat brain as previously reported (Cummings et al., 1983; Merchenthaler, 1984; Morin et al., 1999; Sawchenko and Swanson, 1990; Swanson et al., 1983). Brain CRF immunoreactivity in colchicine-treated mice shows a distribution in discrete regions in a pattern that generally bears similarity to that of rat brain with some exceptions. In addition, we showed in non-colchicine-treated rats that abdominal surgery activates CRF signaling pathways specifically located in the PVN providing anatomical support for the recruitment of the hypothalamic CRF neurons under conditions of post-operative gastric ileus (Barquist et al., 1996; Bonaz et al., 1994; Taché et al., 1991).

The polyclonal CRF antiserum (CURE ab 200101) characterized for cross-reactivity with other members of the CRF family of peptides showed no cross-reactivity when tested by immunodot blotting and cross-reacted only with urotensin-I by radioimmunoassay. However, by immunohistochemical methods in rat and mouse brain sections, we detected cross-reaction with urotensin-I and partially with r/mUcn 1 and mUcn 2. One previous study showed that an ovine CRF antibody cross-reacted with urotensin-I by enzyme-linked immunosorbent assay (ELISA) but not by radioimmunoassay (RIA) (Beny et al., 1985). The discrepancies could result from the use of different techniques or secondary and tertiary peptide structures in the brain (Skofitsch and Jacobowitz, 1985). The cross-reactivity may not be primarily related to the amino acid homology, because the CRF antiserum does not show cross-reactivity with sauvagine that bears 44% sequence identity with r/m/hCRF, while r/mUcn 1 and mUcn 2 which share 45% and 34 % homology respectively (Reyes et al., 2001; Suda et al., 2004; Vaughan et al., 1995) display partial cross-reactivity by immunohistochemical methods. Studies indicate that the CRF amino acids 4–15 are the key antigenic group resulting in the cross-reactivity with urotensin-I while amino acids 9–15 are important for cross-reactivity with Ucn 1 (Suda et al., 2004). Although urotensin-I is not a mammalian peptide and not expressed in the mouse and rat brain, the high level of cross-reactivity with CRF antibody CURE 200101 indicates that urotensin-I has similar antigenic

properties, which is in keeping with the similar biological actions of CRF and urotensin-I in the rat brain (Negri et al., 1985). This may also hold for the partial cross-reactivity of the CRF antiserum with Ucn 1 and to a smaller extent with Ucn 2. For example, urotensin-I, Ucn 1, Ucn 2 when administered centrally in rats and mice, reduce food intake and gastric emptying *via* interaction with CRF receptors (Britton et al., 1984; Martinez et al., 1998; Martinez et al., 2004; Negri et al., 1985; Spina et al., 1996; Zorrilla et al., 2003).

The cross-reactivity is exemplified by the immunoreactive neurons detected in the EW by present and previous CRF antibodies including rC70 from the Salk Institute (Chung et al., 1987; Cummings et al., 1983; Morin et al., 1999), which most likely reflects Ucn 1-ir neurons. This is supported by the total absence of CRF immunoreactivity after the pre-absorption of the antibody by Ucn 1 peptide. In addition, the EW is well established in the rat and mouse brain to be the dominant nucleus of Ucn 1 expression at both the gene and protein levels while lacking CRF mRNA expression (Bachtell et al., 2002; Bittencourt et al., 1999; Kozicz et al., 1998; Kozicz et al., 2004; Weitemier et al., 2005, present study). Collectively these findings indicate that the CRF immunoreactivity distribution in rat and mouse brains using CRF antibodies, CURE 200101 and rC70 do not only capture signals of CRF peptide, but also to some extent other mammalian CRF family peptides structurally and functionally related namely Ucn 1>Ucn 2. However, the use of the Ucn 1 antibody can be a helpful reference when the distribution of CRF-ir neurons is overlapping with Ucn 1 labeling in addition to assessing CRF vs. Ucns mRNA expression. Indeed, the r/mUcn 1 antibody (CURE ab 2023) that we have generated displays a very selective immunoreactivity for Ucn 1 without cross-reaction with other CRF family peptides (present study). Using this Ucn 1 antibody, we found a distinct distribution of Ucn 1-ir neurons in colchicine-treated rat brain including high expression in the EW similar as previously reported (Bittencourt et al., 1999; Kozicz et al., 1998; Morin et al., 1999).

With regard to the distributions of CRF-ir neurons in the rat brain, some differences have been reported when using antibodies generated by different laboratories (Merchenthaler, 1984; Sakanaka et al., 1987a; Skofitsch and Jacobowitz, 1985; Swanson et al., 1983). Comparing the CURE 200101 CRF antibody with the most widely used CRF-antiserum (rC70, Salk Institute), only a few rat brain areas were stained by rC70 but not by CURE 200101 CRF antibody, namely the nucleus ambiguous and hypoglossal nucleus when the immunostaining was conducted simultaneously in colchicine-treated rats. In the PAG, CRF-ir neurons and fibers were demonstrated previously (Cummings et al., 1983; Merchenthaler, 1984; Sakanaka et al., 1987b; Swanson et al., 1983), except in the ventral-median group of neurons where we found CRF immunoreactivity. This represents CRF specific staining as there is no Ucn 1 perikaria in this cell group (Bittencourt et al., 1999). The PAG is a well-known brain center processing pain signals and other functions (Behbehani, 1995). For instance, some studies showed that CRF acts in the PAG *via* CRF_1 receptors to induce defensive behavior (Borelli and Brandao, 2008; Litvin et al., 2007). The newly identified CRF-ir neurons in the ventral median PAG provide additional anatomical evidence that CRF plays a role in functions involving PAG pathways. We also identified a distinct group of CRF-ir neurons in the lateral mammillary nucleus which has been little studied (Kovacs et al., 1985) and where Ucn 1-ir neurons do not exist (present study). The mammillary body relays signals from the hippocampus to the thalamus associated with emotion and memory (Vann and Aggleton, 2004) which points to a role of CRF in this process that needs to be delineated. Overall, these differences represent only a very small proportion compared to the wide distribution of CRF-ir neurons in rat brain detected by CURE 200101 r/m/h CRF antibody and the commonly used rC70 CRF antibody.

Comparison of CRF immunoreactivity in the brain of naïve mice and rats indicates that while in rats CRF immunostaining is readily observed in cell bodies of several nuclei

namely PVN, CeA, BTS and Barrington's, these were rarely identified in mice indicative of interspecies difference in the immunochemical detectability of CRF-ir neurons. As CRF-ir neurons were found in colchicine-treated mice, the lack of CRF immunoreactivity is unlikely to be related to low sensitivity of the immunolabeling reaction in mice compared with rats but most likely reflects differences in peptide content. Consistent with these findings, one investigation focusing on strain differences in the localization of CRF-ir neurons in CeA of naïve rats and mice, showed numerous CRF-ir cell bodies in rat CeA while they were rarely found in C57BL/6 mice (Asan et al., 2005). The CRF gene expression in the CeA detected by *in situ* hybridization labeling was also lower in mice than in rats (Asan et al., 2005). In the present study, we used colchicine to enhance immunohistochemical detectability of CRF-ir perikaria by blocking axonal transport, and also found that CRF-ir cell bodies are less densely represented in mice both in intensity and area than those in rats with a few exceptions. Taken together, this may be indicative of a lower rate of CRF synthesis in mice than in rats. Whether such a difference may also reflect a higher rate of neuronal transport of the peptide to axon terminals in mice than in rats cannot be excluded. However, we used the same dose of colchicine icv per rat and per mouse while the brain volume of mice is about 4-fold smaller compared to rats. Therefore, it is unlikely that such a difference is linked with the experimental conditions of assessment performed using the same antibody in both species and higher concentration of colchicine/brain in mice than in rats.

Colchicine treatment in mice revealed CRF-ir neurons in specific brain nuclei, such as the lateral septum, BST, PVN, LPB, Barrington's nucleus, superior and inferior olivary nuclei and DMN. CRF-ir fibers in naïve mice were prominent in the median eminence, BST and CeA and moderately stained in the medial preoptic area and several midbrain nuclei while observed less in the pontine and medullary nuclei except the medial parabrachial nucleus, ventrolateral medulla and inferior olivary nuclei. These data expand previous reports in mice focused on individual brain nuclei detecting the presence of CRF immunoreactivity in fibers and/or cell bodies in the median eminence (Hayley et al., 2001), PVN (Westberg et al., 2009; Workman et al., 2008), BST, CeA (Asan et al., 2005; Costine et al., 2010), LPB or medial vestibular nucleus (Westberg et al., 2009). In addition, the locations of CRF-ir neurons overlap mostly with areas containing CRF mRNA in wild type mice and CRF-green fluorescent protein transgenic mice (Alon et al., 2009). Overall, the brain distribution of CRF-ir neurons and fibers in mice closely resembles the occurrence found in the rat under the same conditions. However, our comparative studies also point to noticeable species differences. In mice CRF-ir neurons are more abundant in the lateral septum and external subnucleus of the LPB as well as CRF-ir fibers in the medial parabrachial nucleus compared to rats. In addition, the CRF-ir neurons in the mouse DMN are not present in rats, whereas the numerous CRF-ir neurons in the rat medial preoptic area and DLTg are absent in mouse brains. The lateral septum plays an important role in regulating stress-related behaviors in rodents (Sheehan et al., 2004; Veenema and Neumann, 2007). This nucleus is also reported to contain high density of CRF_1 receptor in an immunohistochemical mapping in mice brain (Chen et al., 2000). Whether the prominent CRF-CRF_1 signaling in the lateral septum may have a bearing with the differential responses to stress particularly in emotional behavior between the two species has to be analyzed in correlative studies. The existence of CRF-ir neurons in the mouse DMN combined with high expression of CRF_1 receptors at the gene and protein levels reported in mice compared to rats (Chen et al., 2000; Van Pett et al., 2000) may suggest a prominent role of CRF-CRF_1 signaling system in the vagal regulation of gastric function in mice. This is supported by studies in CRF overexpressing mice which displayed a 5.6-fold increase in Fos-immunoreactive cell number in the DMN and a 34% increase in gastric emptying compared to wild type mice under conditions of metabolic stress induced by overnight fasting (Stengel et al., 2009). The medial parabrachial nucleus which is involved in sensory taste representation is also endowed with more CRF-ir fibers in

mice than in rats which may indicate a broader influence of sensory information processing in the medial parabrachial nucleus by CRF in mice (Panguluri et al., 2009; Sewards, 2004).

Double immunolabeling of Fos and CRF has provided a useful tool to localize various stress stimuli-induced activation of CRF neurons in specific rat brain areas without colchicine. Therefore, we performed the double immunolabeling of Fos and CRF in the brain of rats after abdominal surgery that was not established before. CRF-containing neurons in the PVN are activated by foot shock or icv injection of interleukin-1β (Rivest and Rivier, 1994), immobilization (Rotllant et al., 2007), restraint stress (Covenas et al., 1993; Crane et al., 2005), maternal separation, swim stress (Desbonnet et al., 2008), and hypotensive challenge (Curtis et al., 2002). In other brain areas, CRF neurons that are activated by immobilization or hypotension include the CeA (Honkaniemi, 1992) and Barrington's nucleus (Curtis et al., 2002) respectively. In the present study, we found that the visceral stressor of abdominal surgery increased Fos-ir neurons by 7.7 folds in the PVN compared to sham exposed to anesthesia alone as monitored 2 h post-surgery/anesthesia. These data are consistent with our previous reports when Fos was assessed in the brain between 1 or 3 h after similar surgery compared to animals exposed to anesthesia alone (Barquist et al., 1996; Bonaz et al., 1994; Stengel et al., 2010). Double immunolabeling showed that Fos co-existed in about 30% of CRF-ir neurons after abdominal surgery although there was a significant 25% decrease in the number of CRF-ir neurons in the PVN that could be linked with the release of hypothalamic CRF in the postoperative period as reported previously (Giuffre et al., 1988; Naito et al., 1991). However, outside of the PVN we did not observe co-localization of Fos and CRF immunoreactivity in the brain nuclei displaying CRF-ir neurons in non-colchicine-treated rats, namely the BST, CeA and Barrington's nucleus where only a few Fos-ir cells were observed after the surgery. The demonstration that CRF-producing neurons in the parvicellular PVN are selectively activated by abdominal surgery combined with the responsiveness of the PVN to CRF to delay gastric emptying and the reversal of delayed gastric emptying post-surgery by central injection of CRF receptor antagonists (Barquist et al., 1996; Monnikes et al., 1992) provide a direct neuroanatomical support for a role of CRF in the PVN as part of the visceral and endocrine responses during the postoperative period (Barquist et al., 1996; Luckey et al., 2003; Taché et al., 1991; Uetsuki et al., 2005). The activation of CRF neurons in the PVN may exert inhibitory effect on vagal efferent neurons in the DMN which regulates gastric emptying. This is supported by neuroanatomical and functional evidence. The PVN CRF-ir neurons project to the dorsal vagal complex (Sawchenko, 1987), icv administration of CRF in rats inhibits Fos expression in the DMN neurons induced by cold stress (Wang et al., 1996) and intracisternal injection of CRF or Ucn 1 inhibits gastric emptying through vagal pathways (Czimmer et al. 2006). However, the present study also indicates that 75% of Fos-ir neurons induced by abdominal surgery are also occurring in non-CRF-ir neurons, indicative that additional neuropeptides or transmitters are activated by abdominal surgery. This is evidenced by our previous studies showing that abdominal surgery performed under similar conditions in rats induced Fos expression in the parvicellular division of the PVN in 33% of oxytocin, 25% of vasopressin (Bonaz et al., 1994) and 9% of nucleobindin-2/nesfatin-1 containing neurons (Stengel et al., 2010).

In summary, we showed that while the principal distribution of CRF-ir was similar in mice and in rats treated with colchicine, there were strain differences as the brain of C56BL/6 mice displays a lesser distribution in both number of areas and density that was more noticeable in hindbrain nuclei, and CRF-ir neurons are not readily detectable in naïve mice compared to rats. This was observed using a newly characterized polyclonal r/m/hCRF antibody CURE 200101 with high titer and partial cross reaction with Ucn 1>Ucn 2 at the immunohistochemical level similar to the other CRF antibody, rC70. This first mapping of CRF-ir neurons and fibers in mice brain will be valuable in the context of behavior studies

using genetic mouse models and targeting selective CRF-ir neurons. The differences of CRF-ir locations in mouse and rat brains such as in the lateral septum and DMN may have implications in their behavior responsiveness to stress and in the vagal regulation of gut function. We also demonstrated that the visceral stressor of abdominal surgery activates 30% of CRF neurons in the PVN in non-colchicine-treated rats. This provides neuroanatomical support for the recruitment of hypothalamic CRF pathways in postoperative gastric ileus as shown by pharmacological interventions with central injection of CRF receptor antagonists (Barquist et al., 1996; Taché et al., 1991).

4. Experimental Procedures

4.1. Animals

Adult male Sprague-Dawley rats (Harlan, San Diego, CA, body weight: 280–350g), C57BL/6 mice (Harlan, body weight: 28–33g) and female New Zealand white rabbits (Harlan, 8 weeks old) were used. Rats and mice were housed 4 animals/cage and rabbits 2/cage under conditions of controlled illumination (12:12-hour light/dark cycle, lights on/off: 06:00 a.m./06:00 p.m.) and temperature (22 ± 2 °C) and fed with a standard diet (Prolab RMH 2500; LabDiet, PMI Nutrition, Brentwood, MO, USA) and tap water *ad libitum*. Animal care and experimental procedures followed institutional ethic guidelines and conformed to the requirements of the federal authority for animal research conduct. All procedures were approved by the Animal Research Committees at Veterans Affairs Greater Los Angeles Healthcare System (animal protocol number 99127-07). In all studies animals were euthanized between 09:00 a.m. and 01:00 p.m.

4.2. Antibody generation and characterization

The antigens were [DTyr^0]r/m/hCRF and [DTyr^0]r/mUcn (Clayton Foundation Laboratories, Salk Institute, La Jolla, CA) synthesized using solid phase methodology (Rivier et al., 2002). The rabbit anti-r/m/h CRF antibody CURE 200101 and anti-r/mUcn 1 antibody (CURE ab 2023) were generated and screened as described before (Sternini et al., 1997). Briefly, the peptides were conjugated to keyhole limpet haemocyanin (Calbiochem, La Jolla, CA) using bisdiazotized benzidine which couples through tyrosine residues. The conjugate was emulsified with an equal volume of complete Freund's adjuvant (Difco La, Detroit, MI) and six rabbits were immunized by intradermal injections. The generated CRF antiserum was screened by ELISA as described before (Sternini et al., 1997) and RIA was performed to test the antibody's specificity by displacement of ^{125}I-[DTyr^0]r/hCRF with CRF family peptides.

4.3. Immunodot blot

Synthetic r/m/hCRF, r/mUcn 1, mUcn 2, mUcn 3, frog sauvagine, fish urotensin-I (Clayton Foundation Laboratories, Salk Institute) and BSA (Sigma-Aldrich, St Louis, MN) were weighed and dissolved in double distilled H_2O to a final concentration of 250 ng/μl. For the dot blot, 2 μl of each were slowly spotted on a nitrocellulose membrane (Invitrogen, Carlsbad, CA) at the center of a pre-drawn grid. The membrane was dried and stained for CRF immunoreactivity. The membrane was incubated in anti-CRF antibody solution diluted 1:10,000 in Tween-tris-buffered saline (TBS) followed by the secondary antibody (anti-rabbit IgG conjugated to alkaline phosphate; Promega, Madison, WI) diluted 1:2000 in Tween-TBS, each for 1 h. The membrane was developed in alkaline phosphatase buffer [100 mM Tris, 100 mM NaCl, and 5 mM $MgCl_2$ (pH 9.5)] containing 0.3% nitroblue tetrazolium solution (vol/vol) and 0.15% 5-bromo-4-chloro-3-indolyl-l-phosphate solution (vol/vol) (Sigma-Aldrich) according to the manufacturer's instructions for 5–10 min. Afterwards, the membrane was dried and scanned.

4.4. Colchicine treatment

Naïve rats (n=4) were anesthetized under ketamine (75 mg/kg, ip; Ketanest, Fort Dodge Laboratories, Fort Dodge, IO, USA) and xylazine (5 mg/kg, ip; Rompun, Mobay, Shawnee, KS, USA) and injected into the lateral brain ventricle (icv) with 20 μg colchicine (Sigma-Aldrich) in 10 μl saline/rat using a Hamilton syringe according to the following coordinates given from bregma: −0.8 mm lateral, −1.5 mm dorsal and −4.5 mm ventral (Paxinos and Watson, 2007). Rats were euthanized by overdose of sodium pentobarbital [70 mg/kg, intraperitoneally (ip); Nembutal®, Abbott Laboratories, Chicago, IL] 2 days after the injection and brains processed for CRF and Ucn 1 immunohistochemistry.

In naïve mice (n=6), acute icv injection was performed as described previously (Martinez et al., 2004) under short isoflurane anesthesia (2–3 min, 4.5% vapor concentration in oxygen; VSS, Rockmart, GA). The injection site was localized at the apex of the equal triangle between the eyes and the back of the head, and cleaned with Povidone-Iodine 10% (Aplicare Inc., Meriden, CT). The skull was punctured manually at the point of least resistance with a 30-gauge needle equipped with a polyethylene tube leaving 3.5–4.0 mm of the needle tip exposed. The needle was attached to a Hamilton syringe and colchicine (20 μg in 5 μl saline/mouse) was injected. Twenty-four hours after the injection, mice were transcardially perfused for brain immunohistochemical processing.

The dose of colchicine was lower (20 μg) than commonly used doses (40–200 μg) to assess neuropeptides immunoreactivity in the brain under condition of axonal transport in rats (Bittencourt et al., 1999; Ceccatelli et al., 1989; Foo et al., 2008; Hurley et al., 2003; Schulz et al., 2007; Stanic et al., 2010) and mice (Hurley et al., 2003; Ibanez-Sandoval et al., 2010; Stanic et al., 2010). This lower dose in our study was aiming to minimize stressful effects on the animals due to the neural toxicity of colchicine. However at such a dose, colchicine may still induce a stress response (Berkenbosch and Tilders, 1988).

4.5. Abdominal surgery

Rats were housed in single cages and fasted overnight (~20 h) with free access to tap water. Between 9:00 and 11:00 a.m., rats (n=5) were exposed to isoflurane (4.5% vapor concentration in oxygen) and abdominal surgery was performed as described before (Stengel et al., 2010). After a median laparotomy (2–3 cm), the cecum was exteriorized, placed in saline-soaked gauze and manipulated between two fingers for 1 min. Thereafter, the cecum was replaced into the abdominal cavity and the peritoneum, muscle and skin were sutured. Anesthesia and surgery lasted for approximately 8 min and animals regained the righting reflex within 2–3 min after removal of isoflurane. The control group (n=5) consisted of rats undergoing anesthesia alone for 8 min. After anesthesia, animals were placed singly in cages without access to food or water until euthanasia by an overdose of sodium pentobarbital (70 mg/kg, ip) 2 h after surgical or sham procedure for transcardial perfusion.

4.6. Brain tissue preparation

The procedure was essentially as previously reported (Wang et al., 1996; Wang et al., 2009). Animals were deeply anesthetized with sodium pentobarbital (70 mg/kg for rats and 100 mg/kg for mice, ip) and perfused transcardially with isotonic saline (0.9% NaCl) followed by 400–500 ml (for rats) or 40–50 ml (for mice) of 4% paraformaldehyde and 14% saturated picric acid in 0.1 M phosphate buffer (PB, pH 7.4). Brains were then removed and dissected, post-fixed in the same fixative overnight at 4°C and then cryoprotected over 24 h in 10% sucrose in 0.1 M phosphate buffer saline (PBS). Coronal sections (25 μm) from prefrontal forebrain to the caudal medulla were cut in a cryostat (Microm International GmbH, Walldorf, Germany) and divided in 3 or 6 sets for rat and 3 for mouse brains.

4.7. Immunohistochemistry

Free-floating brain sections of rats and mice were incubated overnight at 4°C with rabbit polyclonal anti-CRF (1:10,000; CURE ab 200101, UCLA Digestive Diseases Research Center, Los Angeles, CA and rC70, Clayton Foundation Laboratories for Peptide Biology, Salk Institute) and anti-Ucn 1 (1:2,000; CURE ab 2023, UCLA, Digestive Disease Research Center) as primary antibodies. Then, sections were incubated with biotinylated secondary goat anti-rabbit IgG (1:1000, Jackson ImmunoResearch Laboratories Inc. Cat No. 111-067-003; West Grove, PA) followed by the incubation with the avidin-biotin-peroxidase complex (1:200; Vector, Burlingame, CA), and each incubation lasted for 1 h at room temperature. The chromogen was diaminobenzidine tetrachloride (0.025%, Sigma-Aldrich) with hydrogen peroxide (0.01%, Sigma-Aldrich). After staining, sections were mounted, air-dried, dehydrated in ethanol, cleared in xylene and coverslipped.

Specificity of the CRF and Ucn 1 antibodies was assessed by preabsorption with an excess of peptides, r/m/hCRF, r/mUcn 1, mUcn 2, mUcn 3, fish urotensin-I and frog sauvagine (Clayton Foundation Laboratories for Peptide Biology, Salk Institute). This was achieved using r/m/h CRF and other peptides at 10 μg/ml concentration with the CRF antibody diluted at 1:10,000 and 50 μg/ml with the Ucn 1 antibody diluted at 1:2,000 (antigen:antibody ratio: 100:1). The antigen-antibody mixture was incubated for 24 h at 4°C and then used as a working primary antibody, as described above.

CRF immunoreactivity in brain sections was examined by light microscope (Axioscop II, Carl Zeiss, Germany) and images were acquired by a digital camera (Hamamatsu, Bridgewater, NJ) using the image acquisition system SimplePCI (Hamamatsu Corporation, Sewickley, PA). The density of CRF-ir cells in each nucleus or area was determined in at least 5 sections in a field of 100 × 100 μm using a 10× objective with a grid in the ocular of the microscope, and assigned according to a scale of + to ++++ in which "+"corresponds to approximately 1–4 cells, "++" 5–10, "+++" 10–20 and "++++" more than 20 immunoreactive cells.

4.8. Immunohistochemical double labeling for Fos and CRF

Brain sections from rats with abdominal surgery and sham treatment (anesthesia alone) were processed at the same time to assess immunoreactivity of Fos and CRF by two consecutive cycles of immunohistochemical staining. Both anti-Fos (Catalog No. PC#38, Oncogene, Cambridge, MA) and anti-CRF (CURE ab 200101) sera were diluted at 1:10,000. The procedures were the same as above, except for coloration of the Fos antigen and antibody binding products which were enhanced by nickel sulfate as previously described (Wang et al., 2009). Fos and CRF-ir cells were observed by light microscopy (Axioscop II, Carl Zeiss, Jena, Germany). Cells with dark blue nuclear staining were Fos-ir and cells with brown cytoplasmic staining were CRF-ir.

For quantitative assessment, the number of immunoreactive cells was counted unilaterally in the PVN in 5 sections from −1.56 mm to −1.92 mm from the bregma according to the rat rain atlas (Paxinos and Watson, 2007), which corresponds to the area containing most of the subdivisions including the dorsomedial parvicellular portion where the majority of CRF-ir neurons are located (Sawchenko et al. 1987, present study). A Plexiglas grid with 10 × 10 squares was placed in one of the eyepieces of the microscope for counting cells. The coordinates for the BST (dorsal part of the lateral subdivision where majority of CRF-ir neurons are located) are 0.24 to −0.24 mm, CeA (lateral subdivision) −1.92 to −3.12 mm and Barrington nucleus −9.00 to −9.48 mm from the bregma (Paxinos and Watson, 2007). Images were acquired by a digital camera (Hamamatsu, Bridgewater, NJ) using the image acquisition system SimplePCI (Hamamatsu Corporation, Sewickley, PA, USA).

The average number of single- or double-labeled Fos-ir and CRF-ir cells/section of each animal was calculated unilaterally as described before (Goebel et al., 2009; Wang et al., 2009). Since no consecutive sections were used for the detection of the same neuronal marker, no corrections for double counting were applied. The investigator was blinded to the treatment.

4.9. Statistical analysis

The average number of single or double labeled Fos-ir and CRF-ir cells/section derived from the total number of sections analyzed for each nucleus was determined for each animals and used to calculate the mean value/group. Data were analyzed by unpaired Student *t-test*. Differences were considered significant when $p < 0.05$. Data are expressed as mean ± SEM.

Highlights

- The new rat/mouse CRF antibody CURE 200101 displays high quality of immunostaining
- CRF neurons in mice show a few distinct brain distributions compared with rats
- Abdominal surgery increases Fos expression selectively in rat hypothalamic CRF neurons

Supplementary Material

Refer to Web version on PubMed Central for supplementary material.

Acknowledgments

This work was supported by the National Institute of Diabetes and Digestive and Kidney Diseases; Center Grant DK-P30 41301 (Animal and Antibody Cores), R01 Grant DK-33061 (YT), P50 AR 049550 (YT, LW), VA Career Scientist Award (YT) and VA Merit Award (YT). We thank Drs. Wylie Vale and Jean Rivier (Clayton Foundation Laboratories for Peptide Biology, Salk Institute, La Jolla, CA) for the generous supply of PBL rC70 CRF antibody as well as CRF and related peptides. We are grateful to Mrs. Honghui Liang, Mr. Robert Kui and the late Ms. Helen Wong for their excellent technical support.

References

1. Alon T, Zhou L, Perez CA, Garfield AS, Friedman JM, Heisler LK. Transgenic mice expressing green fluorescent protein under the control of the corticotropin-releasing hormone promoter. Endocrinology. 2009; 150:5626–5632. [PubMed: 19854866]
2. Asan E, Yilmazer-Hanke DM, Eliava M, Hantsch M, Lesch KP, Schmitt A. The corticotropin-releasing factor (CRF)-system and monoaminergic afferents in the central amygdala: investigations in different mouse strains and comparison with the rat. Neuroscience. 2005; 131:953–967. [PubMed: 15749348]
3. Bachtell RK, Tsivkovskaia NO, Ryabinin AE. Alcohol-induced c-Fos expression in the Edinger-Westphal nucleus: pharmacological and signal transduction mechanisms. J Pharmacol. Exp. Ther. 2002; 302:516–524. [PubMed: 12130710]
4. Bale TL, Vale WW. CRF and CRF receptors: role in stress responsivity and other behaviors. Annu. Rev. Pharmacol. Toxicol. 2004; 44:525–557. [PubMed: 14744257]
5. Barquist E, Bonaz B, Martinez V, Rivier J, Zinner MJ, Taché Y. Neuronal pathways involved in abdominal surgery-induced gastric ileus in rats. Am. J. Physiol. 1996; 270:R888–R894. [PubMed: 8967419]
6. Behbehani MM. Functional characteristics of the midbrain periaqueductal gray. Prog. Neurobiol. 1995; 46:575–605. [PubMed: 8545545]

7. Beny JL, Corder R, Nieuwenhuijzen Kruseman AC, Lowry PJ. CRF immunoreactive peptides in the human hypophysis: a cautionary note. Peptides. 1985; 6:661–667. [PubMed: 2999732]
8. Berkenbosch F, Tilders FJ. Effect of axonal transport blockade on corticotropin-releasing factor immunoreactivity in the median eminence of intact and adrenalectomized rats: relationship between depletion rate and secretory activity. Brain Res. 1988; 442:312–320. [PubMed: 2453250]
9. Bittencourt JC, Vaughan J, Arias C, Rissman RA, Vale WW, Sawchenko PE. Urocortin expression in rat brain: evidence against a pervasive relationship of urocortin-containing projections with targets bearing type 2 CRF receptors. J. Comp. Neurol. 1999; 415:285–312. [PubMed: 10553117]
10. Bonaz B, Plourde V, Taché Y. Abdominal surgery induces Fos immunoreactivity in the rat brain. J. Comp Neurol. 1994; 349:212–222. [PubMed: 7860779]
11. Borelli KG, Brandao ML. Effects of ovine CRF injections into the dorsomedial, dorsolateral and lateral columns of the periaqueductal gray: a functional role for the dorsomedial column. Horm. Behav. 2008; 53:40–50. [PubMed: 17920596]
12. Britton DR, Hoffman DK, Lederis K, Rivier J. A comparison of the behavioral effects of CRF, sauvagine and urotensin I. Brain Res. 1984; 304:201–205. [PubMed: 6611193]
13. Ceccatelli S, Villar MJ, Goldstein M, Hokfelt T. Expression of c-Fos immunoreactivity in transmitter-characterized neurons after stress. Proc. Natl. Acad. Sci. U. S. A. 1989; 86:9569–9573. [PubMed: 2512584]
14. Chen Y, Brunson KL, Muller MB, Cariaga W, Baram TZ. Immunocytochemical distribution of corticotropin-releasing hormone receptor type-1 (CRF(1))-like immunoreactivity in the mouse brain: light microscopy analysis using an antibody directed against the C-terminus. J. Comp. Neurol. 2000; 420:305–323. [PubMed: 10754504]
15. Chung RY, Mason P, Strassman A, Maciewicz R. Edinger-Westphal nucleus: cells that project to spinal cord contain corticotropin-releasing factor. Neurosci. Lett. 1987; 83:13–19. [PubMed: 2831475]
16. Coste SC, Murray SE, Stenzel-Poore MP. Animal models of CRH excess and CRH receptor deficiency display altered adaptations to stress. Peptides. 2001; 22:733–741. [PubMed: 11337086]
17. Costine BA, Oberlander JG, Davis MC, Penatti CA, Porter DM, Leaton RN, Henderson LP. Chronic anabolic androgenic steroid exposure alters corticotropin releasing factor expression and anxiety-like behaviors in the female mouse. Psychoneuroendocrinology. 2010; 35:1473–1485. [PubMed: 20537804]
18. Covenas R, de LM, Cintra A, Bjelke B, Gustafsson JA, Fuxe K. Coexistence of c-Fos and glucocorticoid receptor immunoreactivities in the CRF immunoreactive neurons of the paraventricular hypothalamic nucleus of the rat after acute immobilization stress. Neurosci. Lett. 1993; 149:149–152. [PubMed: 8474689]
19. Crane JW, French KR, Buller KM. Patterns of neuronal activation in the rat brain and spinal cord in response to increasing durations of restraint stress. Stress. 2005; 8:199–211. [PubMed: 16236624]
20. Cummings S, Elde R, Ells J, Lindall A. Corticotropin-releasing factor immunoreactivity is widely distributed within the central nervous system of the rat: an immunohistochemical study. J Neurosci. 1983; 3:1355–1368. [PubMed: 6345725]
21. Curtis AL, Bello NT, Connolly KR, Valentino RJ. Corticotropin-releasing factor neurones of the central nucleus of the amygdala mediate locus coeruleus activation by cardiovascular stress. J. Neuroendocrinol. 2002; 14:667–682. [PubMed: 12153469]
22. Czimmer J, Million M, Taché Y. Urocortin 2 acts centrally to delay gastric emptying through sympathetic pathways while CRF and urocortin 1 inhibitory actions are vagal dependent in rats. Am. J. Physiol. 2006; 290:G511–G518.
23. Delic S, Streif S, Deussing JM, Weber P, Ueffing M, Holter SM, Wurst W, Kuhn R. Genetic mouse models for behavioral analysis through transgenic RNAi technology. Genes Brain Behav. 2008; 7:821–830. [PubMed: 18518923]
24. Desbonnet L, Garrett L, Daly E, McDermott KW, Dinan TG. Sexually dimorphic effects of maternal separation stress on corticotrophin-releasing factor and vasopressin systems in the adult rat brain. Int. J Dev. Neurosci. 2008; 26:259–268. [PubMed: 18367364]

25. Elliott E, Ezra-Nevo G, Regev L, Neufeld-Cohen A, Chen A. Resilience to social stress coincides with functional DNA methylation of the Crf gene in adult mice. Nat. Neurosci. 2010; 13:1351–1353. [PubMed: 20890295]
26. Fekete EM, Zorrilla EP. Physiology, pharmacology, and therapeutic relevance of urocortins in mammals: ancient CRF paralogs. Front Neuroendocrinol. 2007; 28:1–27. [PubMed: 17083971]
27. Foo KS, Brismar H, Broberger C. Distribution and neuropeptide coexistence of nucleobindin-2 mRNA/nesfatin-like immunoreactivity in the rat CNS. Neuroscience. 2008; 156:563–579. [PubMed: 18761059]
28. Giuffre KA, Udelsman R, Listwak S, Chrousos GP. Effects of immune neutralization of corticotropin-releasing hormone, adrenocorticotropin, and beta-endorphin in the surgically stressed rat. Endocrinology. 1988; 122:306–310. [PubMed: 2826112]
29. Goebel M, Stengel A, Wang L, Taché Y. Restraint stress activates nesfatin-1-immunoreactive brain nuclei in rats. Brain Res. 2009; 1300:114–124. [PubMed: 19733157]
30. Hauger RL, Grigoriadis DE, Dallman MF, Plotsky PM, Vale WW, Dautzenberg FM. International Union of Pharmacology. XXXVI. Current Status of the Nomenclature for Receptors for Corticotropin-Releasing Factor and Their Ligands. Pharmacol. Rev. 2003; 55:21–26. [PubMed: 12615952]
31. Hayley S, Staines W, Merali Z, Anisman H. Time-dependent sensitization of corticotropin-releasing hormone, arginine vasopressin and c-fos immunoreactivity within the mouse brain in response to tumor necrosis factor-alpha. Neuroscience. 2001; 106:137–148. [PubMed: 11564424]
32. Honkaniemi J. Colocalization of peptide- and tyrosine hydroxylase-like immunoreactivities with Fos-immunoreactive neurons in rat central amygdaloid nucleus after immobilization stress. Brain Res. 1992; 598:107–113. [PubMed: 1362516]
33. Hurley DL, Birch DV, Almond MC, Estrada IJ, Phelps CJ. Reduced hypothalamic neuropeptide Y expression in growth hormone- and prolactin-deficient Ames and Snell dwarf mice. Endocrinology. 2003; 144:4783–4789. [PubMed: 12960004]
34. Ibanez-Sandoval O, Tecuapetla F, Unal B, Shah F, Koos T, Tepper JM. Electrophysiological and morphological characteristics and synaptic connectivity of tyrosine hydroxylase-expressing neurons in adult mouse striatum. J Neurosci. 2010; 30:6999–7016. [PubMed: 20484642]
35. Kainu T, Honkaniemi J, Gustafsson JA, Rechardt L, Pelto-Huikko M. Colocalization of peptide-like immunoreactivities with glucocorticoid receptor- and Fos-like immunoreactivities in the rat parabrachial nucleus. Brain Res. 1993; 615:245–251. [PubMed: 8364734]
36. Kovacs M, Lengvari I, Liposits Z, Vigh S, Schally AV, Flerko B. Corticotropin-releasing factor (CRF)-immunoreactive neurons in the mammillary body of the rat. Cell Tissue Res. 1985; 240:455–460. [PubMed: 3922623]
37. Kozicz T, Korosi A, Korsman C, Tilburg-Ouwens D, Groenink L, Veening J, Van Der GJ, Roubos E, Olivier B. Urocortin expression in the Edinger-Westphal nucleus is down-regulated in transgenic mice over-expressing neuronal corticotropin-releasing factor. Neuroscience. 2004; 123:589–594. [PubMed: 14706771]
38. Kozicz T, Yanaihara H, Arimura A. Distribution of urocortin-like immunoreactivity in the central nervous system of the rat. J. Comp. Neurol. 1998; 391:1–10. [PubMed: 9527535]
39. Litvin Y, Pentkowski NS, Blanchard DC, Blanchard RJ. CRF type 1 receptors in the dorsal periaqueductal gray modulate anxiety-induced defensive behaviors. Horm. Behav. 2007; 52:244–251. [PubMed: 17540371]
40. Lovejoy DA, Balment RJ. Evolution and physiology of the corticotropin-releasing factor (CRF) family of neuropeptides in vertebrates. Gen. Comp. Endocrinol. 1999; 115:1–22. [PubMed: 10375459]
41. Lovejoy DA, Rotzinger S, Barsyte-Lovejoy D. Evolution of complementary peptide systems: teneurin C-terminal-associated peptides and corticotropin-releasing factor superfamilies. Ann. N. Y. Acad. Sci. 2009; 1163:215–220. [PubMed: 19456342]
42. Luckey A, Wang L, Jamieson PM, Basa NR, Million M, Czimmer J, Vale W, Taché Y. Corticotropin-releasing factor receptor 1-deficient mice do not develop postoperative gastric ileus. Gastroenterology. 2003; 125:654–659. [PubMed: 12949710]

43. Martinez V, Barquist E, Rivier J, Taché Y. Central CRF inhibits gastric emptying of a nutrient solid meal in rats: the role of CRF2 receptors. Am. J. Physiol. 1998; 274:G965–G970. [PubMed: 9612279]
44. Martinez V, Wang L, Rivier J, Grigoriadis D, Taché Y. Central CRF, urocortins and stress increase colonic transit via CRF1 receptors while activation of CRF2 receptors delays gastric transit in mice. J. Physiol. 2004; 556:221–234. [PubMed: 14755002]
45. Merchenthaler I. Corticotropin releasing factor (CRF)-like immunoreactivity in the rat central nervous system. Extrahypothalamic distribution. Peptides. 1984; 5 Suppl 1:53–69. [PubMed: 6384954]
46. Merchenthaler I, Vigh S, Petrusz P, Schally AV. Immunocytochemical localization of corticotropin-releasing factor (CRF) in the rat brain. Am. J Anat. 1982; 165:385–396. [PubMed: 6760710]
47. Monnikes H, Schmidt BG, Raybould HE, Taché Y. CRF in the paraventricular nucleus mediates gastric and colonic motor response to restraint stress. Am. J. Physiol. 1992; 262:G137–G143. [PubMed: 1733259]
48. Morgan JI, Curran T. Stimulus-transcription coupling in the nervous system: involvement of the inducible proto-oncogenes fos and jun. Annu. Rev. Neurosci. 1991; 14:421–451. [PubMed: 1903243]
49. Morin SM, Ling N, Liu XJ, Kahl SD, Gehlert DR. Differential distribution of urocortin- and corticotropin-releasing factor-like immunoreactivities in the rat brain. Neuroscience. 1999; 92:281–291. [PubMed: 10392850]
50. Mundy WR, Tilson HA. Neurotoxic effects of colchicine. Neurotoxicology. 1990; 11:539–547. [PubMed: 2284057]
51. Naito Y, Fukata J, Tamai S, Seo N, Nakai Y, Mori K, Imura H. Biphasic changes in hypothalamo-pituitary-adrenal function during the early recovery period after major abdominal surgery. J Clin. Endocrinol. Metab. 1991; 73:111–117. [PubMed: 1646214]
52. Negri L, Noviello L, Noviello V. Effects of sauvagine, urotensin I and CRF on food intake in rats. Peptides. 1985; 6 Suppl 3:53–57. [PubMed: 3879535]
53. Olschowka JA, O'Donohue TL, Mueller GP, Jacobowitz DM. The distribution of corticotropin releasing factor-like immunoreactive neurons in rat brain. Peptides. 1982; 3:995–1015. [PubMed: 6984756]
54. Owens MJ, Nemeroff CB. Physiology and pharmacology of corticotropin-releasing factor. Pharmacol. Rev. 1991; 43:425–473. [PubMed: 1775506]
55. Panguluri S, Saggu S, Lundy R. Comparison of somatostatin and corticotrophinreleasing hormone immunoreactivity in forebrain neurons projecting to taste-responsive and nonresponsive regions of the parabrachial nucleus in rat. Brain Res. 2009; 1298:57–69. [PubMed: 19699720]
56. Paxinos, G.; Watson, C. The rat brain in stereotaxic coordinates. Orlando: Academic Press; 2007.
57. Petrusz P, Merchenthaler I, Maderdrut JL, Heitz PU. Central and peripheral distribution of corticotropin-releasing factor. Fed. Proc. 1985; 44:229–235. [PubMed: 3871410]
58. Pollak DD, Rey CE, Monje FJ. Rodent models in depression research: classical strategies and new directions. Ann. Med. 2010; 42:252–264. [PubMed: 20367120]
59. Reyes TM, Lewis K, Perrin MH, Kunitake KS, Vaughan J, Arias CA, Hogenesch JB, Gulyas J, Rivier J, Vale WW, Sawchenko PE. Urocortin II: A member of the corticotropin-releasing factor (CRF) neuropeptide family that is selectively bound by type 2 CRF receptors. Proc. Natl. Acad. Sci. U. S. A. 2001; 98:2843–2848. [PubMed: 11226328]
60. Rivest S, Rivier C. Stress and interleukin-1 beta-induced activation of c-fos, NGFI-B and CRF gene expression in the hypothalamic PVN: comparison between Sprague-Dawley, Fisher-344 and Lewis rats. J Neuroendocrinol. 1994; 6:101–117. [PubMed: 8025563]
61. Rivier J, Gulyas J, Kirby D, Low W, Perrin MH, Kunitake K, DiGruccio M, Vaughan J, Reubi JC, Waser B, Koerber SC, Martinez V, Wang L, Taché Y, Vale W. Potent and long-acting corticotropin releasing factor (CRF) receptor 2 selective peptide competitive antagonists. J Med. Chem. 2002; 45:4737–4747. [PubMed: 12361401]

62. Rotllant D, Nadal R, Armario A. Differential effects of stress and amphetamine administration on Fos-like protein expression in corticotropin releasing factor-neurons of the rat brain. Dev. Neurobiol. 2007; 67:702–714. [PubMed: 17443818]
63. Sakanaka M, Shibasaki T, Lederis K. Corticotropin releasing factor-like immunoreactivity in the rat brain as revealed by a modified cobalt-glucose oxidase-diaminobenzidine method. J Comp Neurol. 1987a; 260:256–298. [PubMed: 3497182]
64. Sakanaka M, Shibasaki T, Lederis K. Improved fixation and cobalt-glucose oxidase-diaminobenzidine intensification for immunohistochemical demonstration of corticotropin-releasing factor in rat brain. J Histochem. Cytochem. 1987b; 35:207–212. [PubMed: 3491848]
65. Sawchenko, P.; Swanson, LW. Organization of CRF immunoreactive cells and fibers in the rat brain: immunohistochemical studies. In: De Souza, EB.; Nemeroff, CB., editors. Cortico-Releasing Factor: Basic and Clinical Studies of A Neuropeptide. CRC Press; 1990.. p. 29-51.
66. Sawchenko PE. Evidence for differential regulation of corticotropin-releasing factor and vasopressin immunoreactivities in parvocellular neurosecretory and autonomic-related projections of the paraventricular nucleus. Brain Res. 1987; 437:253–263. [PubMed: 3325130]
67. Sawchenko PE, Imaki T, Potter E, Kovacs K, Imaki J, Vale W. The functional neuroanatomy of corticotropin-releasing factor. Ciba Found. Symp. 1993; 172:5–21. [PubMed: 8491094]
68. Sawchenko PE, Swanson LW, Vale WW. Corticotropin-releasing factor: co-expression within distinct subsets of oxytocin-, vasopressin-, and neurotensin-immunoreactive neurons in the hypothalamus of the male rat. J. Neurosci. 1984; 4:1118–1129. [PubMed: 6609226]
69. Schulz S, Stumm R, Hollt V. Immunofluorescent identification of neuropeptide B-containing nerve fibers and terminals in the rat hypothalamus. Neurosci. Lett. 2007; 411:67–71. [PubMed: 17067739]
70. Seasholtz AF, Bourbonais FJ, Harnden CE, Camper SA. Nucleotide sequence and expression of the mouse corticotropin-releasing hormone gene. Mol. Cell Neurosci. 1991; 2:266–273. [PubMed: 19912808]
71. Sewards TV. Dual separate pathways for sensory and hedonic aspects of taste. Brain Res. Bull. 2004; 62:271–283. [PubMed: 14709342]
72. Sheehan TP, Chambers RA, Russell DS. Regulation of affect by the lateral septum: implications for neuropsychiatry. Brain Res. Brain Res. Rev. 2004; 46:71–117. [PubMed: 15297155]
73. Skofitsch G, Jacobowitz DM. Distribution of corticotropin releasing factor-like immunoreactivity in the rat brain by immunohistochemistry and radioimmunoassay: comparison and characterization of ovine and rat/human CRF antisera. Peptides. 1985; 6:319–336. [PubMed: 3875839]
74. Spina M, Merlo-Pich E, Chan RK, Basso AM, Rivier J, Vale W, Koob GF. Appetite-suppressing effects of urocortin, a CRF-related neuropeptide. Science. 1996; 273:1561–1564. [PubMed: 8703220]
75. Stanic D, Kuteeva E, Nylander I, Hokfelt T. Characterization of CGRP protein expression in "satellite-like" cells and dendritic arbours of the mouse olfactory bulb. J Comp Neurol. 2010; 518:770–784. [PubMed: 20058222]
76. Stengel A, Goebel M, Million M, Stenzel-Poore MP, Kobelt P, Monnikes H, Tach H, Taché Y, Wang L. Corticotropin-releasing factor-overexpressing mice exhibit reduced neuronal activation in the arcuate nucleus and food intake in response to fasting. Endocrinology. 2009; 150:153–160. [PubMed: 18787020]
77. Stengel A, Goebel M, Wang L, Taché Y. Abdominal surgery activates nesfatin-1 immunoreactive brain nuclei in rats. Peptides. 2010; 31:263–270. [PubMed: 19944727]
78. Stengel A, Taché Y. Corticotropin-releasing factor signaling and visceral response to stress. Exp. Biol. Med. (Maywood.). 2010; 235:1168–1178. [PubMed: 20881321]
79. Sternini C, Wong H, Wu SV, De GR, Yang M, Reeve J Jr, Brecha NC, Walsh JH. Somatostatin 2A receptor is expressed by enteric neurons, and by interstitial cells of Cajal and enterochromaffin-like cells of the gastrointestinal tract. J Comp Neurol. 1997; 386:396–408. [PubMed: 9303425]
80. Suda T, Kageyama K, Sakihara S, Nigawara T. Physiological roles of urocortins, human homologues of fish urotensin I, and their receptors. Peptides. 2004; 25:1689–1701. [PubMed: 15476936]

81. Swanson LW, Sawchenko PE, Rivier J, Vale WW. Organization of ovine corticotropin-releasing factor immunoreactive cells and fibers in the rat brain: an immunohistochemical study. Neuroendocrinology. 1983; 36:165–186. [PubMed: 6601247]
82. Taché Y, Barquist E, Stephens RL, Rivier J. Abdominal surgery and trephination induced delay in gastric emptying is prevented by intracisternal injection of CRF antagonist in the rat. J. Gastrointest. Motil. 1991; 3:19–25.
83. Taché Y, Bonaz B. Corticotropin-releasing factor receptors and stress-related alterations of gut motor function. J. Clin. Invest. 2007; 117:33–40. [PubMed: 17200704]
84. Uetsuki N, Segawa H, Mayahara T, Fukuda K. The role of CRF1 receptors for sympathetic nervous response to laparotomy in anesthetized rats. Brain Res. 2005; 1044:107–115. [PubMed: 15862795]
85. Van Pett K, Viau V, Bittencourt JC, Chan RK, Li HY, Arias C, Prins GS, Perrin M, Vale W, Sawchenko PE. Distribution of mRNAs encoding CRF receptors in brain and pituitary of rat and mouse. J. Comp Neurol. 2000; 428:191–212. [PubMed: 11064361]
86. Vann SD, Aggleton JP. The mammillary bodies: two memory systems in one? Nat. Rev. Neurosci. 2004; 5:35–44. [PubMed: 14708002]
87. Vaughan J, Donaldson C, Bittencourt J, Perrin MH, Lewis K, Sutton S, Chan R, Turnbull AV, Lovejoy D, Rivier C. Urocortin, a mammalian neuropeptide related to fish urotensin I and to corticotropin-releasing factor. Nature. 1995; 378:287–292. [PubMed: 7477349]
88. Veenema AH, Neumann ID. Neurobiological mechanisms of aggression and stress coping: a comparative study in mouse and rat selection lines. Brain Behav. Evol. 2007; 70:274–285. [PubMed: 17914259]
89. Wang L, Cardin S, Martinez V, Taché Y. Intracerebroventricular CRF inhibits cold restraint-induced c-fos expression in the dorsal motor nucleus of the vagus and gastric erosions in rats. Brain Res. 1996; 736:44–53. [PubMed: 8930307]
90. Wang L, Martinez V, Larauche M, Taché Y. Proximal colon distension induces Fos expression in oxytocin-, vasopressin-, CRF- and catecholamines-containing neurons in rat brain. Brain Res. 2009; 1247:79–91. [PubMed: 18955037]
91. Weitemier AZ, Tsivkovskaia NO, Ryabinin AE. Urocortin 1 distribution in mouse brain is strain-dependent. Neuroscience. 2005; 132:729–740. [PubMed: 15837134]
92. Westberg L, Sawa E, Wang AY, Gunaydin LA, Ribeiro AC, Pfaff DW. Colocalization of connexin 36 and corticotropin-releasing hormone in the mouse brain. BMC. Neurosci. 2009; 10:41. [PubMed: 19405960]
93. Workman JL, Trainor BC, Finy MS, Nelson RJ. Inhibition of neuronal nitric oxide reduces anxiety-like responses to pair housing. Behav. Brain Res. 2008; 187:109–115. [PubMed: 17928072]
94. Zorrilla EP, Taché Y, Koob GF. Nibbling at CRF receptor control of feeding and gastrocolonic motility. Trends Pharmacol. Sci. 2003; 24:421–427. [PubMed: 12915052]

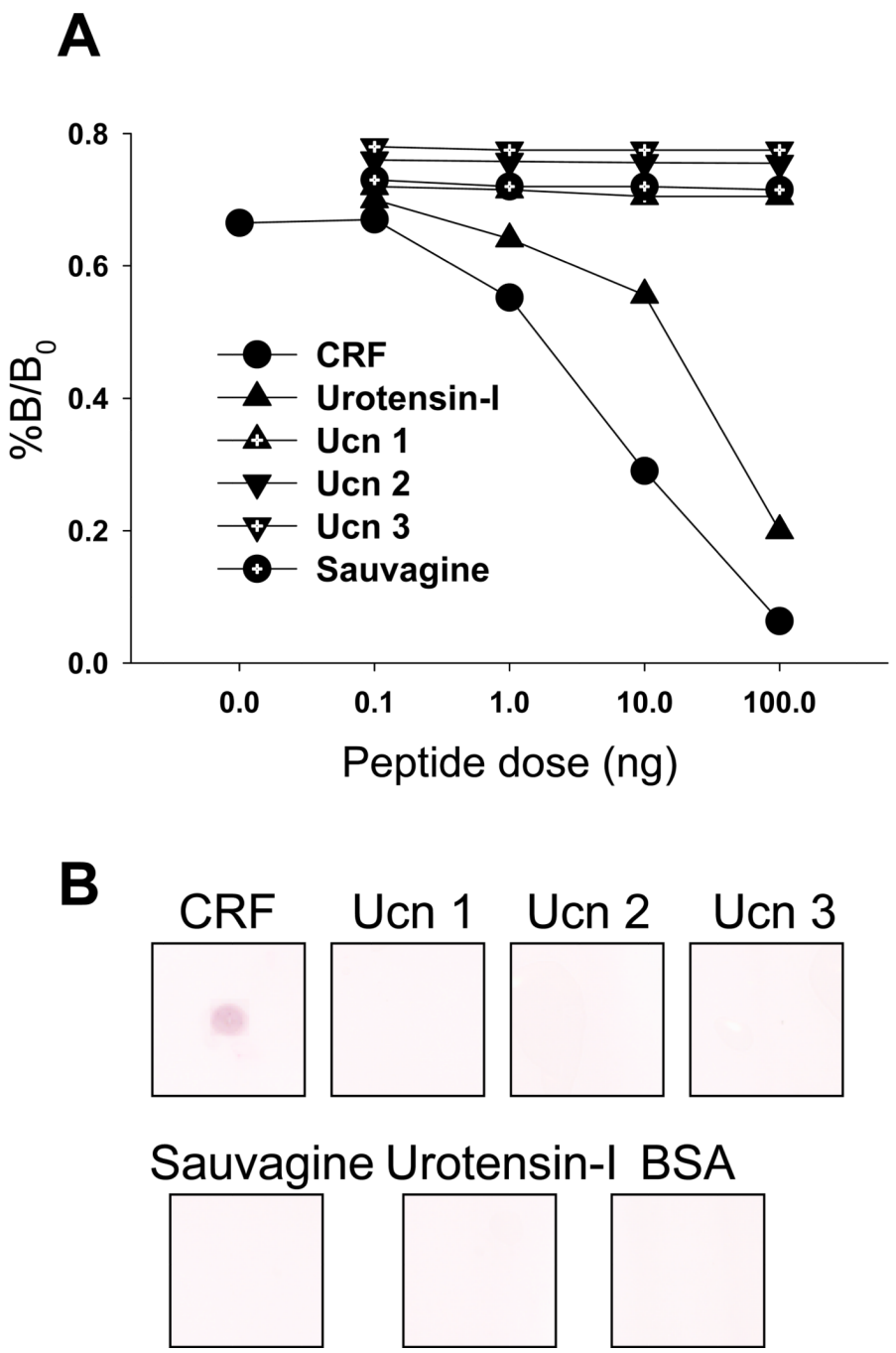

Fig. 1.

Characterization of the rabbit anti-CRF antibody CURE 200101. A. r/m/hCRF inhibits ^{125}I-CRF binding to the polyclonal r/m/hCRF antibody by radioimmunoassay. There is cross-reactivity with fish urotensin-I (ID_{50}: 30 ng/ml) but not with r/mUcn 1, mUcn 2, mUcn 3 or frog sauvagine. B. Immunodot blotting of CRF peptide family members with the rabbit CRF antibody CURE 200101 (1:10,000). On each square of a nitrocellulose membrane 500 ng of peptides (r/m/h CRF, r/mUcn 1, mUcn 2, mUcn 3, fish urotensin-I, frog sauvagine) and bovine serum albumin (BSA) were spotted and the membrane stained according to standard procedures. The CRF antibody selectively recognizes r/m/hCRF but not the other peptides or BSA.

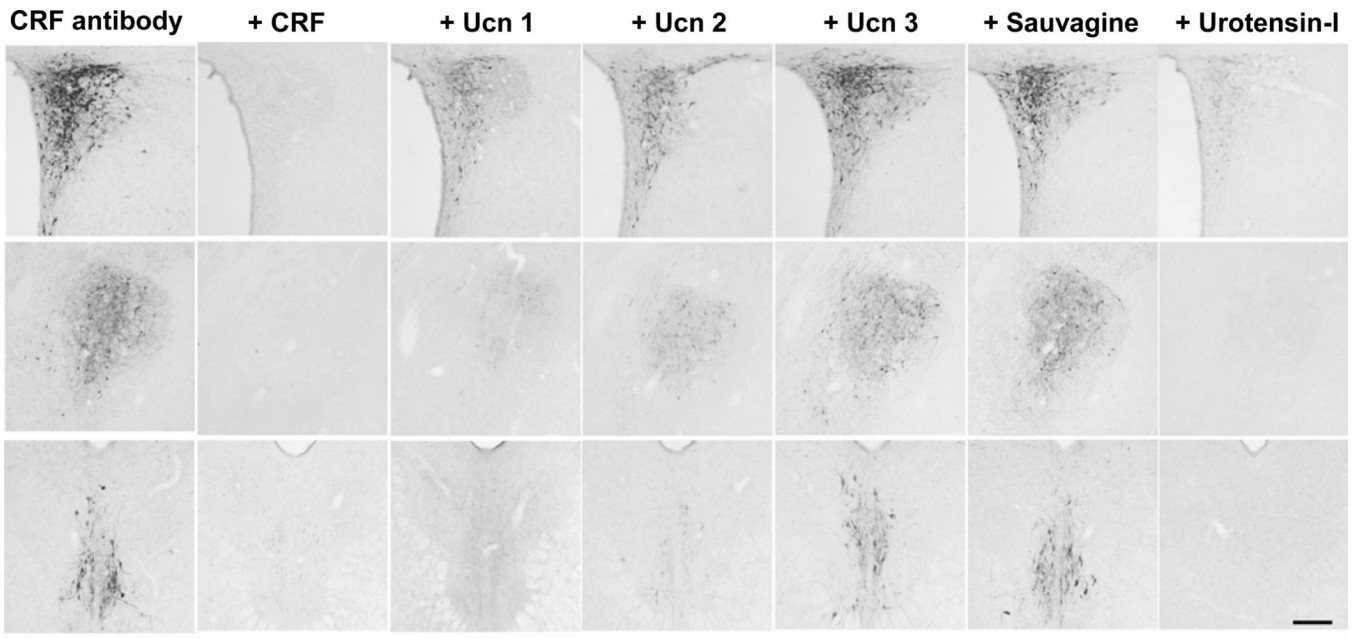

Fig. 2.

Photomicrographs of the hypothalamic paraventricular nucleus in brain sections of colchicine-treated rats after pre-absorption of CRF antibody CURE 200101 by CRF family peptides (upper row), central nucleus of the amygdala, lateral division (middle row) and Edinger-Westphal nucleus (lower row). The photos in the left column show the sections with CRF immunoreactivity without pre-absorption. The 2^{nd} – 7^{th} columns show sections incubated with the rabbit anti-CRF antibody (1:10,000) pre-absorbed with r/m/h CRF, r/mUcn 1, mUcn 2, mUcn 3, frog sauvagine or fish urotensin-I (10 μg/ml) as indicated on the top of each column. Scale bar = 200 μm.

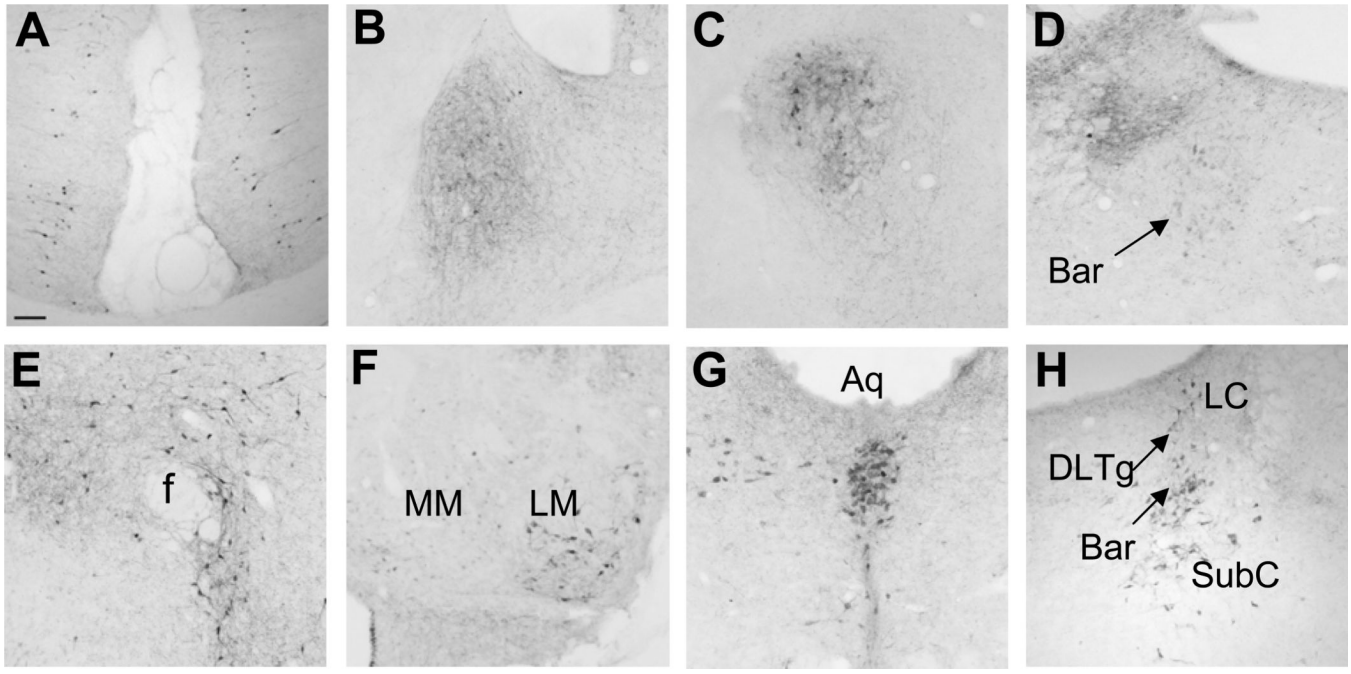

Fig. 3.

Photomicrographs of selective areas showing CRF-ir neurons in non colchicine-treated (A–D) and colchicine-treated rat brains (E–H). CRF immunoreactivity is shown in the cingulate cortex (A), bed nucleus of the stria terminalis, lateral division, dorsal part (B), central nucleus of the amygdala, lateral division (C), and Barrington's nucleus (D), posterior perifornical area (E), lateral mammillary nucleus (F), ventral-median periaqueductal gray (G), and dorsal lateral tegmental area and subcoeruleus nucleus (H). Scale bar in A = 100 μm for all the panels. Abbreviations: Aq: aqueduct; f: fornix; Bar: Barrington's nucleus; DLTg: dorsal lateral tegmental area; MM: medial mammillary nucleus; ML: lateral mammillary nucleus; LC: locus coeruleus; SubC: subcoeruleus nucleus.

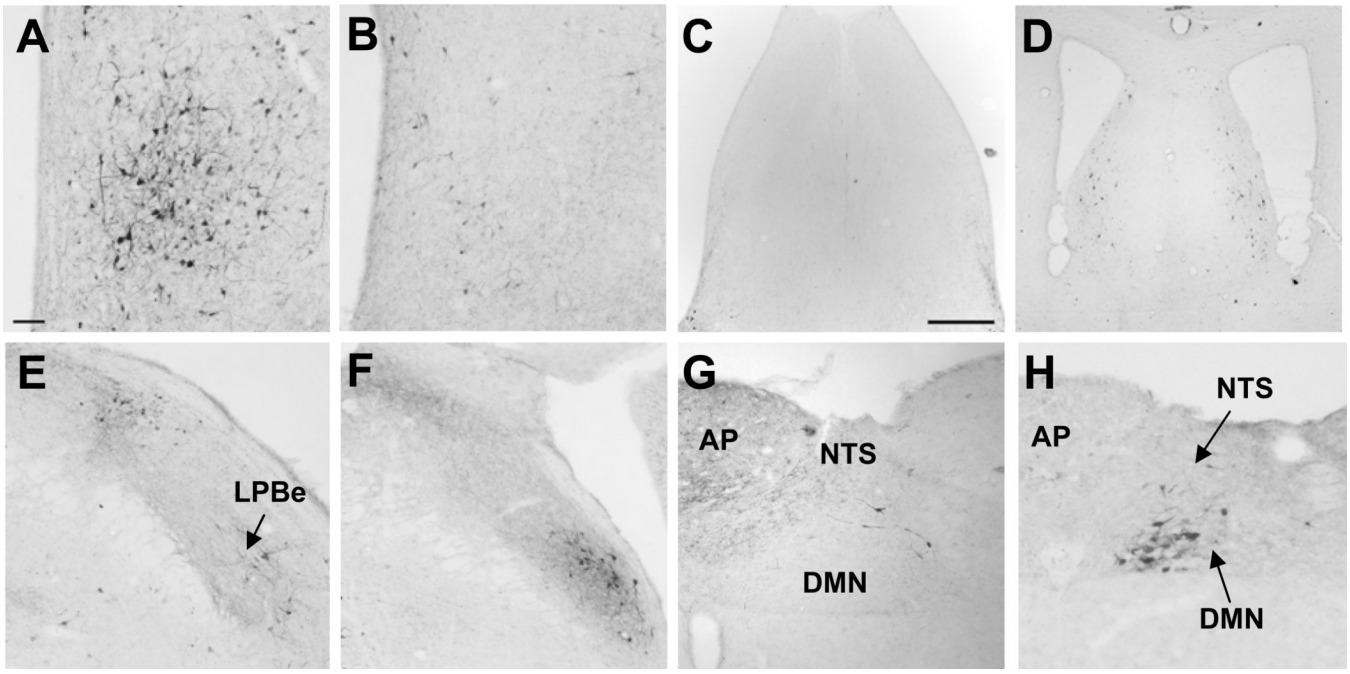

Fig. 4.

Photomicrographs of CRF-ir neurons in selective areas with difference between rat (A, C, E, G) and mouse (B, D, F, H) brains that were colchicine-treated. CRF immunoreactivity in the medial preoptic area (A, B), lateral septal nucleus (C, D), lateral parabrachial nucleus (E, F) and dorsal motor vagal complex (G, H). Scale bar in A = 100 μm except the bar in C = 500 μm for C and D. Other abbreviations: AP: area postrema, DMN: dorsal motor nucleus of the vagus, NTS: nucleus of solitary tract, LPBe: external subnucleus of the lateral parabrachial nucleus.

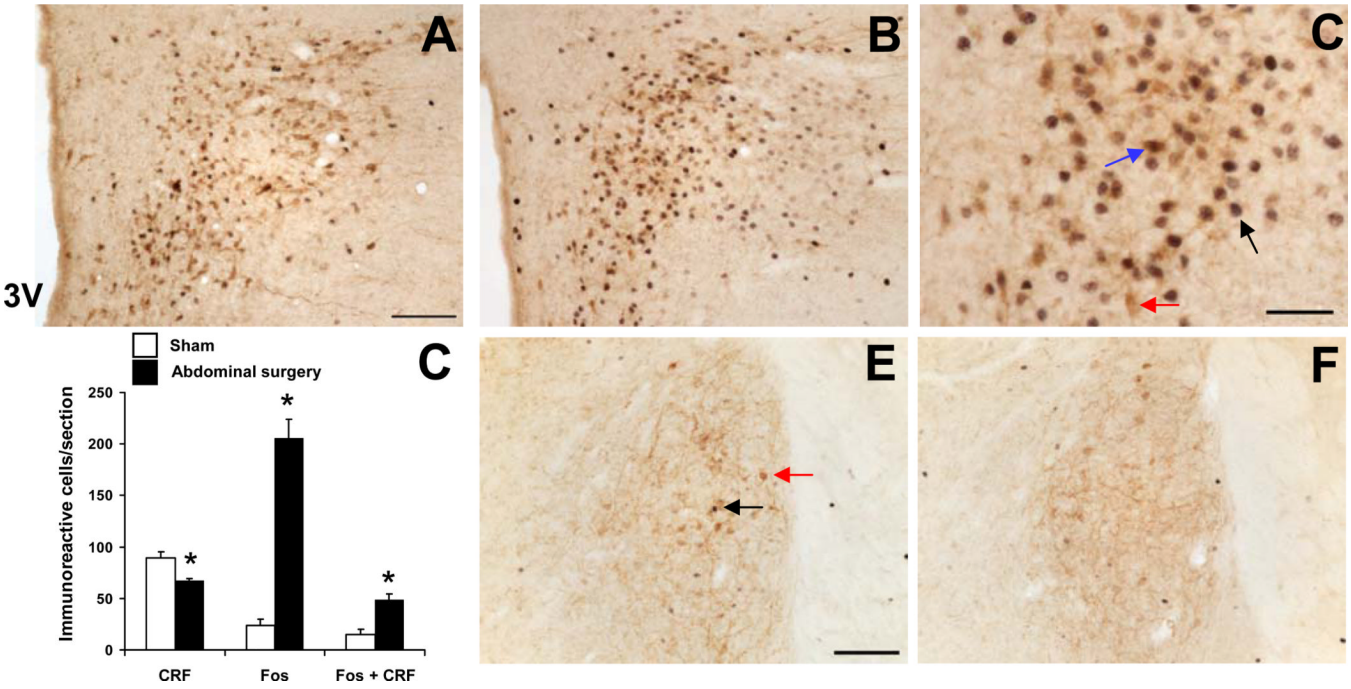

Fig. 5.

Double immunohistochemical staining for Fos (dark blue nuclei) and CRF (brown cytoplasm) in the rat paraventricular nucleus (PVN) in sham treatment (A) and 2 h after abdominal surgery (B, C). C shows a higher magnification of neurons with Fos immunoreactivity co-localizing with CRF immunoreactivity. Black arrows indicate Fos-ir, red CRF-ir and blue double-labeled neurons. The scale bars in A and E represent 100 μm, and 50 μm for C. Unilateral cell count/section in the parvicellular PVN (D) expressed as mean ± SEM of 5 rats/group. * $p < 0.05$ *vs* sham. Other abbreviations: 3V: third brain ventricle.

Table 1

Distributions of CRF immunoreactivity in rat and mouse brain assessed by CRF antibody (CURE 200101). Neurons were labeled in colchicine-treated and fibers in non-treated animal brains.

Brain Structure	Neurons		Fibers	
	Rat	Mouse	Rat	Mouse
Forebrain				
Cortex	++	+	+	+
Nucleus of diagonal band	−	+	+	+
Lateral septum	±	++	+	+
Subfornical organ	−	−	++	+
Interstitial nucleus of posterior limb of the anterior commissure, lateral part	−	−	+++	++
Bed nucleus of the stria terminalis Amygdala	+++	++	+++	+++
Anterior cortical nucleus	−	−	+++	+
Central nucleus	++	+	++	+++
Amygdalostriatal transition area	−	−	+	−
Thalamus				
Paraventricular thalamic nucleus	−	−	+	+
Medial genicular nucleus	+	+	+	+
Hypothalamus				
Lateral preoptic area	−	−	+	+
Medial preoptic area	++	−	++	++
Suprachiasmatic nucleus	+	−	+	+
Periventricular area	+	+	+	+
Supraoptic nucleus	+	−	+	+
Paraventricular nucleus	++++	++++	+	+
Perifornical area	++	+	++	+
Lateral hypothalamic area	++	+	++	+
Dorsomedial hypothalamic nucleus	+	−	+++	+
Arcuate nucleus	+	−	++++	+
Median eminence	−	−	++	++++
Medial mammillary nucleus	−	−	−	+
Lateral mammillary nucleus	++	±	++	+
Midbrain				
Periaqueductal gray	+	−	−	++
Edinger-Westphal nucleus	++	++	++	−
Substantia nigra, lateral part	−	−	++	++
Ventral tegmental area	+	−	++	++
Interfascicular nucleus	+	+	+	++
Superior colliculi	+	−	+	+
Rostral linear raphe nucleus	+	−	++	+
Dorsal raphe	±	−	+	++
Midbrain reticular formation	+	−	++	+

Brain Structure	Neurons		Fibers	
	Rat	Mouse	Rat	Mouse
Cerebellum (climbing and mossy fibers)	−	−	++	++
Pons				
Lateral parabrachial nucleus (central & external subnuclei)	+	++	++	++
Medial parabrachial nucleus	−	−	−	++
Barrington's nucleus	++	++	+	−
Dorsal tegmental nucleus	−	−	+	−
Dorsal lateral tegmental area	+++	−	++	+
Locus coeruleus	±	−	+	+
Subcoeruleus nucleus	+	−	++	−
Superior olivary nucleus	++	++	+	+
Medulla				
Raphe magnus	−	−	+	+
Raphe pallidus	−	−	++	+
Raphe obscurus	+	−	−	−
Medial vestibular nucleus	++	−	+	+
Pre-hypoglossal nucleus	+	+	++	+
Area postrema	−	−	++	+
Nucleus of the solitary tract	+	+	−	+
Dorsal motor nucleus of the vagus	−	++	+	−
Ventrolateral medulla	−	−	+	++
Lateral reticular formation	++	−	+	+
External cuneate nucleus	+	−	++	+
Inferior olivary nucleus	++	++	−	++
Ectotrigeminal nucleus	+	−	−	−

"±" not every animal's brain section, "+" approximately 1–4 cells, "++" 5–10, "+++" 10–20 and "++++" >20 immunoreactive cells in a 100 μm×100 μm area of an ocular grid when the objective was 10×. For the density of immunoreactive fibers: ++++ as in the median eminence (Fig. 4G), +++ as in the BST (Fig. 4A), ++++ and ++ as more and less dense respectively than that in the BST, and + as sparse. Colchicine-treated mice, n=6, other groups n = 4.